

Field theory of self-organized fractal etching

Andrea Gabrielli^{1,2}, Miguel A. Muñoz³, and Bernard Sapoval^{2,4}.

¹*INFM - Unità di Roma 1 and Dip. Fisica, Università "La Sapienza", P.le A. Moro, 2, 00185 - Roma, Italy*

²*Laboratoire de la Physique e la Matière Condensée, Ecole Polytechnique- CNRS, 91128 Palaiseau, France*

³*Instituto de Física Teórica y Compt. Carlos I, Universidad de Granada, Facultad de Ciencias, 18071-Granada, Spain.*

⁴*Centre de Mathématiques et de leurs Applications, Ecole Normale Supérieure - CNRS, 94140 Cachan, France*

(November 27, 2018)

We propose a phenomenological field theoretical approach to the chemical etching of a disordered-solid. The theory is based on a recently proposed dynamical etching model. Through the introduction of a set of Langevin equations for the model evolution, we are able to map the problem into a field theory related to isotropic percolation. To the best of the authors knowledge, it constitutes the first application of field theory to a problem of chemical dynamics. By using this mapping, many of the etching process critical properties are seen to be describable in terms of the percolation renormalization group fixed point. The emerging field theory has the peculiarity of being “self-organized”, in the sense that without any parameter fine-tuning, the system develops fractal properties up to certain scale controlled solely by the volume, V , of the etching solution. In the limit $V \rightarrow \infty$ the upper cut-off goes to infinity and the system becomes scale invariant. We present also a finite size scaling analysis and discuss the relation of this particular etching mechanism with Gradient Percolation. Finally, the possibility of considering this mechanism as a new generic path to self-organized criticality is analyzed, with the characteristics of being closely related to a real physical system and therefore more directly accessible to experiments.

PACS numbers: 64.60Ak, 81.65Cf

I. INTRODUCTION

Corrosion of solids is an everyday phenomenon of evident practical importance [1]. The recent development of theoretical tools for the study of disordered systems and fractals in the context of statistical mechanics [2–5] has triggered an outburst of activity in this subject.

When an etching solution is put in contact with a disordered etchable solid, the solution corrodes the weak parts of the solid surface, while the hard, stronger, parts stay uncorroded. During this process new regions of the solid, both hard and weak, are discovered and come into contact with the etching solution. As corrosion proceeds the etching power of the solution may diminish: indeed, if the etchant is consumed in the reaction, etching becomes more and more unlikely until, finally, the solution is so impoverished and the solid surface so hardened that the corrosion process is arrested. At that moment all solid points in contact with the solution are too hard to be etched by the weakened etching solution. One of the most interesting aspects of this type of phenomenon is that the final solid-liquid interface has, in general, a fractal geometry, at least up to a certain scale [3–6]. This is precisely the qualitative phenomenology observed in a nice experiment on pit corrosion of aluminum thin films [7].

Recently, a simple dynamical model of etching, capturing the aforementioned phenomenology, has been proposed [8,9]. This model has been studied using both computational and analytical tools in [9], and from these studies strong evidence has been provided that the frac-

tal properties of the solid surface, once the dynamics has stopped, are related to isotropic percolation. In principle, this is not an obvious result; in fact, at first sight, one could think that the interface should be anisotropic as there is a preferential direction in which the solution advances by etching the solid.

The purpose of this paper is to provide further theoretical evidence that indeed the critical behavior of the model dynamics is related to isotropic percolation. We also extend the previous relation to spatial dimensions larger than $d = 2$. To this aim, we shall first review (section 2) two known percolation models that will be useful in the forthcoming discussion: (i) dynamical percolation, and (ii) gradient percolation (GP).

Afterwards (section 3), we will define the dynamical etching model [8,9] in a circular (spherical) geometry, and will derive a phenomenological field theory for it (section 4). From the analysis of this field theory the parallelism with percolation will be set up in a rather clear way, and this will provide further theoretical evidence on the connection between etching and percolation phenomena.

The approach presented in this paper will allow us to study the system *self-organization* from a field theoretical point of view, and to verify that, in certain limit, the system is self-driven to the neighborhood of a critical point without need of any parameter fine-tuning. This is a new path to self-organized criticality [10] as will be discussed in the last section.

II. TWO PERCOLATION MODELS

In this section we review two different well-known percolation models that will be useful in the discussion of the etching processes under consideration.

A. Dynamical Percolation

Dynamical percolation is a model proposed for the study of the propagation of epidemics in a population, and/or for the analysis of forest fires. It is defined as follows [12,13]. Let us consider a regular square lattice; at each site there is a variable that can be in one of three possible states (we borrow the language from epidemiology [14]): (i) infected sites, (ii) healthy sites susceptible to be infected, and (iii) immune sites (non susceptible to be re-infected). At time $t = 0$ a localized seed of infected sites is located at the center of an otherwise empty (healthy) lattice. The dynamics proceeds in discrete time steps either by parallel or by sequential updating as follows: at each time-step every infected site can infect a (healthy) randomly chosen neighbor with probability p or, alternatively, heal and become immune to reinfection with complementary probability $1 - p$. Any system state with no infected site is an *absorbing configuration*, i.e., a configuration in which the system can get trapped and from which it cannot escape [15,16]. It is clear that depending on the value of p the epidemics generated by the initial infection seed will either spread in the lattice (for large values of p) or die out (for small values of p). In all cases, the epidemics will leave behind a cluster of (healed) immune sites, infinite or finite respectively for the two aforementioned cases. Separating the two previous phases, there is a critical value of p , $0 < p_c < 1$, at which the epidemics propagates marginally, leaving behind a fractal cluster of immunized sites. It can be shown using field theoretical tools (see below) that this is a percolation cluster [12,13]. In this way we have a dynamical model which at criticality reproduces the (static) properties of standard percolation. Needless to say, the dynamical properties of the dynamical percolation equation, do not correspond to any known property of static percolation.

The dynamical percolation model can be cast into the following Langevin equation [12,13] (or equivalently into a field theory [17,18]):

$$\partial_t \rho(\mathbf{x}, t) = \mu \rho(\mathbf{x}, t) - \alpha \rho(\mathbf{x}, t) \int_0^t dt' \rho(\mathbf{x}, t') + \nabla^2 \rho(\mathbf{x}, t) + \sqrt{\rho(\mathbf{x}, t)} \eta(\mathbf{x}, t) \quad (1)$$

where μ (the “mass” in a field theoretical language”) and $\alpha > 0$ are constants, $\rho(\mathbf{x}, t)$ an activity field describing at a coarse grained level the density of infected sites, and $\eta(\mathbf{x}, t)$ a Gaussian white noise. Note the multiplicative nature of the noise, because of which the state $\rho(\mathbf{x}, t) = 0$

defines an absorbing state, i.e. $\partial_t \rho(\mathbf{x}, t) = 0$. Note also the presence of a non-Markovian term, that constitutes the key difference between this equation and the Reggeon field theory, characteristic of many other systems with absorbing states. This non-Markovian term stems from the existence of immunized sites, of which the system keeps indelible memory [12,13].

The field theoretical and renormalization group analysis of Eq.(1) can be found in the literature [13]. The critical dimension is $d_c = 6$, and the exponents, calculated in an epsilon expansion, coincide with the well known values for percolation calculated using other techniques [19]. Apart from the static exponents, also a dynamical exponent z can be derived from this analysis of dynamical percolation [13].

B. Gradient Percolation

Gradient percolation [20] (GP) is defined in the following way: let us consider a bidimensional rectangular lattice of lateral sizes L and h respectively, as shown in Fig. 1.

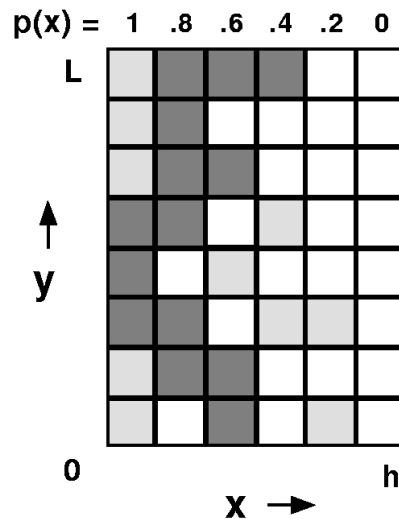


FIG. 1. Schematic representation of the Gradient Percolation model. In this case: $L = 8$ and $h = 5$. Grey (white) rectangles represent occupied (empty) sites. In darker grey we indicate the surface of the connected cluster of occupied sites. This surface has fractal dimension $D_f = 7/4$ up to the characteristic thickness $\sigma \sim \nabla p^{-1/D_f}$.

An occupation probability given by $p(x) = 1 - x/h$ is assigned to sites in column x ; this defines a transversal constant gradient, $\nabla p = 1/h$ for the occupation probability. Then, at each lattice site (x, y) a random number $r(x, y) \in [0, 1]$, extracted from an homogeneous distribution, and representing the site reluctance to be occupied,

is assigned. All sites with $r(x, y) < p(x)$ are declared occupied, while the remainings are empty. At the first column, $x = 0$, all sites are occupied, while there is zero occupancy at the last one, $x = h$ (see Fig. 1). After identifying all sites as occupied or empty, one detects two connected regions (clusters): one (leftmost) with a majority of occupied sites possibly surrounding "lakes" of empty sites, and another one (rightmost sea) possibly surrounding islands. Separating these two regions there is an interface (the frontier of the connected cluster of occupied sites; it corresponds to the dark sites in figure 1). The average position of this interface can be shown to be at the square lattice site percolation threshold, p_c [20,21]. In fact, gradient percolation has been used as a computational tool to obtain accurate values of percolation thresholds in different geometries by identifying the average position of the interface in sufficiently large lattices [20]. In the case that we are considering, the fractal dimension of the interface, $D_f = 7/4$, can be identified as the hull fractal dimension of the critical percolating cluster in a two-dimensional lattice [21]. There is an upper cut-off up to which this fractal behavior is observed; it is fixed by the width σ which, in its turn, is determined by h , and therefore by ∇p . It can be shown using percolation theory that

$$\sigma \sim \nabla p^{-\alpha_\sigma} \quad (2)$$

where $\alpha_\sigma = 1/D_f$ [9,20,22]. In order to have a well defined percolation system, with negligible finite size effects, the limit $L \gg \sigma$ has to be used. In this way, the length h , determining the value of σ , is the parameter that controls the finite size effects; the "thermodynamic limit" corresponds to $h \rightarrow \infty$ and $L \rightarrow \infty$ with both limits taken in the proper way [9]. One can also estimate the variation of p from on the leftmost to the rightmost extremes of the wandering interface, Δp :

$$\Delta p \sim \nabla p^{-\alpha_p}. \quad (3)$$

The identity $\Delta p = \sigma * \nabla p = \sigma/h$ imposes the following scaling relation among exponents: $\alpha_p = 1 - \alpha_\sigma$, and therefore,

$$\alpha_p = \frac{D_f - 1}{D_f}. \quad (4)$$

Let us observe that gradient percolation can also be defined in a circular geometry, in which the gradient changes with the radial distance to the origin, and the cut-off is determined by the width of the roughly circular crown in which the interface is inscribed.

Summarizing, in this section, we have reviewed two well-known percolation models. Dynamical percolation is a model that, at its critical point, generates dynamically a percolation cluster. On the other hand, gradient percolation is a static model, in which an interface appears with the same hull fractal dimension of the percolation cluster, but with no intrinsic dynamics defined.

III. DYNAMICAL ETCHING MODEL

Having introduced the previous two percolation models, we go ahead by reviewing the dynamical etching model (DEM) at the focus of our study [8,9]. It is defined by the following ingredients (see Figure 2).

(i) The random solid is mimicked by a two-dimensional square lattice of finite linear width L and depth Y (Y can be arbitrarily large, or even infinite). Periodic boundary conditions in the finite direction are imposed, leading to a cylindrical geometry.

(ii) A random quenched number $r_i \in [0, 1]$ (extracted from a uniform distribution), assigned to each solid site i , represents the site resistance to etching.

(iii) The etching solution occupies a fixed volume V and is initially in contact with the solid through the bottom boundary, as depicted in Fig. 2, defining a solid-solution interface advancing on average in the upward direction.

The solution contains an initial number $N_{et}(0)$ of dissolved etchant molecules. Its concentration at time t is $C(t) = N_{et}(t)/V$. It is assumed that the etching power of the solution $p(t)$ is proportional to $C(t)$. Without loss of generality the proportionality constant can be fixed to unity. Following [8], we assume that etchant particles diffuse infinitely fast in the solution (at least much faster than the characteristic time scale of etching) and, hence, $p(t)$ is taken as spatially homogeneous, i.e., the etching power does not depend on the spatial position in the solution.

At each discrete time-step all solid sites located at the solid surface and satisfying $r_i < p(t)$ are dissolved (see Fig. 2), i.e., they are removed from the solid, and a particle of etchant is consumed for each dissolved site, reducing in this manner the total etching power.

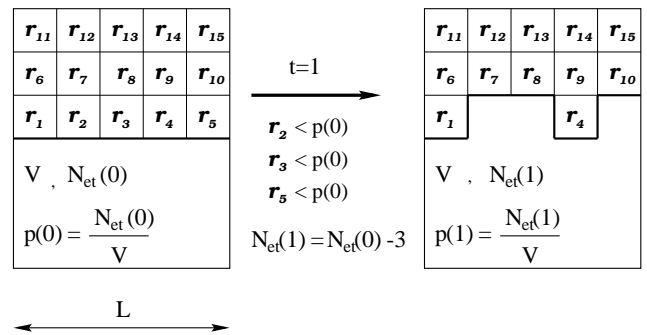


FIG. 2. Schematic representation of the dynamical etching model in "cylindrical" geometry before and after the first time-step. At this first time-step the (active) sites in contact with the solution are $i = 1, 2, 3, 4, 5$, but only 2,3,5 have a resistance lower than the etching power $p(0)$ and then are corroded. At the next time step new sites come in contact with the solution (the whole second row if the solution etches also in diagonal direction). The etching power diminishes because of the consumption of etchant particles. Consequently sites 1, 4 stay uncorroded forever.

Calling $n(t)$ the number of dissolved solid sites (or equivalently the number of consumed etchant particles) at time-step t , and $N(t) = \sum_{t'=0}^t n(t')$ the total number of etched solid sites up to time t , one can write

$$p(t+1) = p(t) - \frac{n(t)}{V} = p(0) - \frac{N(t)}{V}. \quad (5)$$

As $p(t+1) \leq p(t)$, a site having endured the etching attack at time t will also resist at any time $t' > t$ [11]. Furthermore, as a consequence of the corrosion process at time t , $m(t)$ new solid sites, previously in the solid bulk, come into contact with the solution at time $t+1$. Note that they are the sole candidates for corrosion at the next time-step. Finally, since the solution has the possibility to detach finite solid islands, the global solid surface is composed both by the surfaces of the detached islands, and by the set of solid sites separating the solution from the bulk. This interface is called the *corrosion front*. A more detailed description of the model phenomenology can be found in [9]. Here we simply summarize the main features of the corrosion front at the arrest time t_f . They are well represented by GP with $\nabla p \sim L/V$:

(i) the corrosion front shows fractal features with $D_f \simeq 1.75$ up to a characteristic scale (front thickness) σ ;

(ii) $\sigma \sim (L/V)^{-1/D_f}$;

(iii) $p_c - p(t_f) \sim (L/V)^{-\alpha_p}$, with $\alpha_p \simeq (D_f - 1)/D_f$ (therefore, in the right thermodynamic limit $p(t_f) \rightarrow p_c$).

Let us introduce here a slight geometrical modification of the DEM which makes more clear the connection to dynamical percolation. Instead of considering a cylindrical geometry with the etchant solution invading the cylinder from the bottom (as in Fig. 2), we consider a flat infinite lattice, in which the volume V of the etching solution is poured at time $t = 0$ at an arbitrarily chosen central site as schematically shown in Fig. 3. The volume V of the etching solution is constant. Observe that with this geometry the model has some clear analogies with dynamical percolation. The main difference is that, in the spherical DEM, the control parameter (the corroding or infecting probability) is not a constant but decreases in time as the etching process proceeds. As in cylindrical geometry, the dynamics can be roughly divided into two regimes [9]: a *smooth* one when $p(t)$ is much larger than p_c , and a *critical* one when $p(t)$ approaches p_c . In the smooth regime, fluctuations around the average behavior are small while in the critical regime fluctuations dominate the dynamics [8]. Indeed, at early time-steps, the etching power being sufficiently larger than p_c , it is simple to show [9] that the corrosion front is an approximate expanding circumference centered at the origin, and the number of new solid sites coming into contact with the solution at time t satisfies the approximate relation $m(t) \simeq 2\pi R(t)$, where $R(t)$ is the maximal radius reached by the corrosion up to time t . As the etchant power is reduced, the corrosion front becomes rougher and rougher, until the dynamics is finally arrested (see Fig. 3).

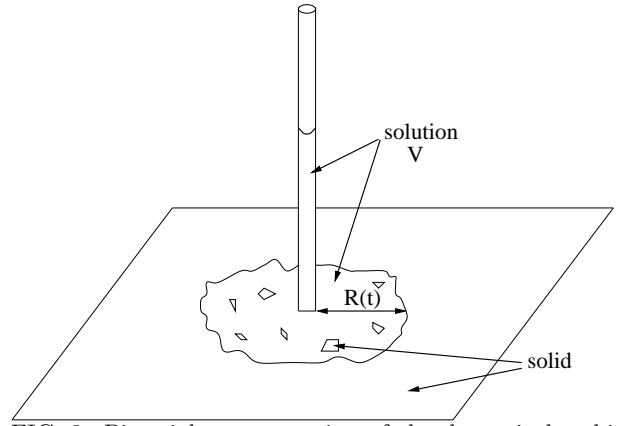


FIG. 3. Pictorial representation of the dynamical etching model in “spherical” geometry.

Since in the smooth regime $m(t) \gg 1$, we can write $n(t) \simeq p(t)m(t)$. Hence, within this approximation, it is possible to write down the following equation:

$$p(t+1) \simeq p(t) - \frac{2\pi R(t)p(t)}{V}. \quad (6)$$

Since in this regime obviously $R(t) \propto t$, we can write Eq. 6 in a differential form as follows:

$$\frac{dp(t)}{dt} \simeq -\frac{2\pi t}{V}p(t), \quad (7)$$

whose solution is

$$p(t) \simeq p(0) \exp(-\pi t^2/V). \quad (8)$$

From this, the characteristic time of the dynamics is seen to be proportional to \sqrt{V} ; i.e. the etching power of the solution reaches the value p_c in a time t_c proportional to \sqrt{V} . Moreover, as $R(t) \propto t$, at the cross-over between the smooth and the critical regime (i.e. when $p(t) \simeq p_c$) the solution reaches a distance $R_c \simeq \sqrt{V}$ from the origin. By differentiating this expression we conclude that the gradient of values of p at which different sites have been corroded in the radial direction is proportional to R/V . Finally, as $R(t_c) \propto \sqrt{V}$, the gradient ∇p at t_c is proportional to $1/\sqrt{V}$. In this way, in analogy with the cylindrical case, we expect that the geometrical properties of the final corrosion front are well represented by GP where the gradient of p is dynamically generated. Replacing ∇p with $1/\sqrt{V}$, the scaling relations studied for gradient percolation can be extended to the present case. The previous description is valid only for the smooth regime, i.e. up to the time at which $p(t) \approx p_c$. However, since the critical regime is shorter than the smooth one, we have $t_f \sim R(t_f) \sim \sqrt{V}$, where $R(t_f)$ is the average radius of the final corrosion front, and the previous estimations remain valid. In order to check that also in the critical regime the radial gradient of the solution etching power is given by R/V , it is sufficient to assume that during this regime the corrosion front changes from a quite smooth geometry to a rougher one, with a final

thickness σ . Because of the much shorter duration of the critical regime one has $\sigma \ll R(t_f)$. In this way, during the critical regime the solution etches a number of solid sites proportional to $\sigma R(t_f)$. Therefore, from Eq. (5), the variation of the etching power in this regime in average is $\Delta p \sim \sigma R(t_f)/V$.

In conclusion, we have defined a spherical version of the DEM, and seen its connection with gradient percolation: given the time-diminution of p , the system generates dynamically a spatial gradient of the values of p at which the different sites were etched. Let us finally emphasize that if, after the process is arrested, more etchant solution is added then the process continues until it is stopped again at a value of p around p_c . In this way the disordered solid plays the role of a chemical buffer. In the next section we present a more theoretical treatment allowing us to draw even more precise connections between DEM and percolation theory.

IV. PHENOMENOLOGICAL FIELD THEORY

In order to construct a field theoretical description for the dynamical etching model, a possibility would be to write down the master equation defining the dynamics and then (using a Poissonian transformation [23,24] or alternatively a Fock-space formalism [25]), derive a generating functional [18]. Instead of following that strategy, we prefer here to present a phenomenological set of stochastic Langevin equations describing the model at a mesoscopic scale. This direct approach, “à la Landau”, based on the analysis of the main symmetries and conservation laws of the discrete model, has proven very efficient in describing many other systems related to percolation, directed percolation and, in general, systems with absorbing states [13,16].

Let us consider the following three different local densities or coarse-grained fields:

- $s(\mathbf{x}, t)$ describing the local density of material susceptible to be etched at any time after t . In the discrete model there are two types of sites contributing to this density: (i) bulk solid sites and (ii) “fresh” interface sites i.e., solid sites freshly arrived to the solid-liquid interface (susceptible to be etched at the next time-step).
- $q(\mathbf{x}, t)$ is the local density of passivated and inert material. In the microscopic model this is the density of interface sites having already resisted an etching trial, i.e., immune or not-susceptible to be corroded at any future time-step.
- $c(\mathbf{x}, t)$ is the local density of corroded and replaced by solution sites, i.e., the local density of etchant.

The mean field equations (rate equations) describing the evolution of the averaged mean values of these magnitudes are:

$$\begin{aligned}\dot{s}(t) &= -\alpha c(t)s(t) \\ \dot{q}(t) &= \alpha(1-p(t))c(t)s(t) \\ \dot{c}(t) &= \alpha p(t)c(t)s(t)\end{aligned}\quad (9)$$

where $p(t)$ is the probability to etch an active site at time t , and α is a positive constant. In what follows, and without loss of generality we fix $\alpha = 1$. The interpretation of the first equation is: in order for the density of susceptible sites to change (decrease) in a region, it is necessary to have locally both a non-vanishing density of etchants and raw solid material susceptible to be etched. This restricts the dynamics to *active* regions, i.e., zones in the interface separating the etchable-solid and the solution, in which non-vanishing local densities of s and of c coexist. Moreover, the second and the third relations in Eq. 9 express the fact that an active site becomes either a c -site, with probability $p(t)$ (the corrosion power at time t), or alternatively, after healing, a q -site with complementary probability $1-p(t)$. Note that, as $\dot{s} + \dot{c} + \dot{q} = 0$, the total number of sites is conserved during the dynamics. It is worth stressing that Eq. (9) captures the fact that sites resisting an etching attempt remain un-corroded indefinitely (as occurs in the microscopic model). In fact, the number of q -sites grows monotonously until the etching process is arrested.

Observe that we have written so far mean field equations in which spatial dependence and fluctuations are not taken under consideration. At this point, it is convenient to introduce an activity field $\rho(\mathbf{x}, t) \equiv c(\mathbf{x}, t)s(\mathbf{x}, t)$ (or $\rho(t) \equiv c(t)s(t)$ as long as spatial dependences are omitted).

From Eq. 9 it follows immediately that

$$\dot{\rho}(t) = -c(t)\rho(t) + p(t)s(t)\rho(t). \quad (10)$$

In order to implement in our theoretical description the diminution of the etching power as the corrosion process proceeds, we write $p(t)$ (analogously to Eq.(4)) as

$$p(t) = p_0 - \frac{N(t)}{V}, \quad (11)$$

where now $N(t) = \int d\mathbf{x}[c(\mathbf{x}, t) - c(\mathbf{x}, 0)]$ is the number of consumed etchant particles up to time t and, as before, V is the solution volume. Integrating in time the equation for c in Eq. 9, integrating then in space, and substituting the result into Eq. 11, we obtain

$$p(t) = p(0) \exp \left[-\frac{1}{V} \int_0^t dt' \int d\mathbf{x}' \rho(\mathbf{x}', t') \right]. \quad (12)$$

Plugging this result into Eq. 10, and re-introducing the spatial dependence of the fields, it is a matter of simple algebra to obtain

$$\begin{aligned}\partial_t \rho(\mathbf{x}, t) &= [p(t)s(\mathbf{x}, 0) - c(\mathbf{x}, 0)]\rho(\mathbf{x}, t) \\ &\quad - \rho(\mathbf{x}, t) \left[\int_0^t dt' (1 - p(t'))\rho(\mathbf{x}, t') \right].\end{aligned}\quad (13)$$

In order to go beyond this mean field description, it is necessary to include properly spatial coupling and fluctuations (as a noise).

- *Spacial coupling*

In principle, the spatial coupling can be taken into account by introducing additional terms into Eq. 13. However, because of the isotropic nature of the local dynamics, terms not invariant under space inversion (as odd derivatives of the fields) are not allowed. Also, terms like $|\nabla\rho(\mathbf{x}, t)|^n$ cannot appear, given the absence of surface tension in the microscopic rules [4]. Therefore, only terms as $\nabla^{2n}\rho(\mathbf{x}, t)$ and higher powers of them are allowed. We introduce in Eq. 13 the only relevant term in the renormalization group optics [18], namely a diffusive coupling $\nabla^2\rho(\mathbf{x}, t)$, that typically appears in continuous descriptions of interacting particle systems. It will be checked *a posteriori* that, as a matter of fact, the omitted terms are irrelevant at criticality.

- *Noise*

In order to introduce properly the noise term, let us consider a small region in which there are k “fresh” surface sites in contact with the solution of etching power p . Since these fresh sites have random independent resistances, the average number of dissolved sites will be $p \cdot k$ and the fluctuation from this average number will be Poissonian, i.e. of order $\sqrt{p \cdot k}$. This implies that in the continuous description fluctuations of $\rho(\mathbf{x}, t)$ are proportional to its square-root. Consequently, a term $\sqrt{\rho(\mathbf{x}, t)}\eta(\mathbf{x}, t)$ has to be added to Eq. 13, with $\eta(\mathbf{x}, t)$ being a Gaussian white noise with zero mean and no spatio-temporal correlations: $\langle \eta(\mathbf{x}, t)\eta(\mathbf{x}', t') \rangle = \delta(\mathbf{x} - \mathbf{x}')\delta(t - t')$. Deviations from gaussianity and higher order corrections can be easily argued to be irrelevant in the renormalization group optics, and therefore are not taken into account. This type of noise, with amplitude proportional to the square-root of the activity field, is characteristic of systems exhibiting a transition from an active to an absorbing phase [24]: let us emphasize that wherever the activity field is zero, the dynamics is stopped [15,16].

Introducing these two new ingredients in Eq.13 one obtains finally

$$\begin{aligned} \partial_t\rho(\mathbf{x}, t) = & [p(t)s(\mathbf{x}, 0) - c(\mathbf{x}, 0)]\rho(\mathbf{x}, t) \\ & - \rho(\mathbf{x}, t) \left[\int_0^t dt' (1 - p(t'))\rho(\mathbf{x}, t') \right] \\ & + \nabla^2\rho(\mathbf{x}, t) + \sqrt{\rho(\mathbf{x}, t)}\eta(\mathbf{x}, t) \end{aligned} \quad (14)$$

up to higher order, irrelevant, terms.

It is worth stressing that even though the microscopic model has originally quenched disorder, it has been possible to describe it in terms of a stochastic equation with

annealed noise. This simplification owes to the fact that every site is tested for corrosion at most once. If it survives, it will stay un-corroded indefinitely, as previously explained. In this way, as every random number is used at most once it has not to be stored, there are no time correlations in the noise and, consequently, a stochastic process with no quenched disorder can be used to cast the discrete model.

It is also important to underline that wherever $\rho(\mathbf{x}, t)$ vanishes, all activity, including fluctuations, ceases in Eq.14. In other words, $\rho(\mathbf{x}, t) = 0$ defines an absorbing state [16,15]. This is just another way of saying that in the microscopic model, whenever there is no contact between the etchable solid and the solution, i.e., when they are separated by an interface of passivated (immune) solid sites, the dynamics is arrested. Continuous descriptions of systems with absorbing states are based on equations for the activity. In the neighborhood of any absorbing state phase transition the activity is small, and series expansions on the activity density (as the ones we have used to arrive at Eq.14) are justified [15,16].

Observe that, apart from the time dependence, of $p(t)$, Eq. 14 is identical to the Langevin equation describing *dynamical percolation* (see Eq. 1) [12,13]. As described above, dynamical percolation is a rather well known dynamical process generating percolation clusters with a characteristic size determined by μ (see Eq. 1). Let us analyze the differences between Eq. 14 and Eq. 1. Particular attention must be paid to the exponential factor in the expression for $p(t)$ (see Eq. 12) absent in dynamical percolation; due to it some of the coefficients in Eq. 14 are time dependent, while their counterparts in Eq. 1 are constants. First we discuss whether this extra time-dependence may affect the critical properties. Note that $p(t)$ does not fluctuate (as verified in simulations in [9]) because it is a smooth function of the integral of the field over all the past time and the whole space. Therefore, it is a deterministically decreasing time-dependent term; or in other words it depends on spatio-temporal integrals of the activity field and not on the local activity field itself. Hence, this term has not critical fluctuations, and does not affect the system critical properties. However, it is crucial in order to characterize the temporal crossover from the active to the absorbing phase. Indeed, as the linear term coefficient in Eq. 14 includes a dependence on $p(t)$, for early times it is positive, corresponding to the fact that for early times the system is in the supercritical regime. As the etching mechanism proceeds, the argument of the exponential in Eq. 12 grows in modulus, and there is a finite time, t_c , at which the linear term coefficient takes its critical value. Immediately after, the process becomes subcritical [26], i.e. it reaches the absorbing phase and, the dynamics tends to be stopped with an exponentially fast rate (i.e. the number of active sites decreases exponentially). Furthermore, as more and more sites are etched, the linear coefficient in Eq. 14 becomes smaller and smaller than its critical value, and the exponential stopping rate is accelerated till a final time t_f , at

which an absorbing (blocking) configuration is reached. Therefore, the main effect of the time-dependent linear term coefficient is that, by continuously diminishing, it drives the system to the neighborhood of the dynamical-percolation-field-theory critical point, but it does not add any new relevant operator that could eventually change the universality class. At this point, it is a matter of simple algebra to verify that all the terms omitted in our derivation are indeed irrelevant at the dynamical percolation, Eq. 1, renormalization group fixed point.

Given the previous discussion, one is allowed to say that Eqs. 12 and 14 define a *self-organized dynamical percolation Langevin equation*: without tuning any parameter the dynamics is arrested in the neighborhood of the percolation critical point, and critical (fractal) properties can be measured up to certain length scale determined solely by the parameter V (which controls the decrease rate of $p(t)$). In the limit $V \rightarrow \infty$ the upper cut-off goes to infinity; i.e., for sufficiently large values of V the point at which the dynamics is stopped occurs at values of p arbitrarily closed to its critical value in Eq. 1.

Observe that the microscopic process is also self-organized: initially $p(t)$ is taken to be super-critical, but it decreases monotonously till it reaches a critical value, and as soon as the sub-critical regime is reached the process is stopped in an exponential way. Therefore, our continuous description reproduces the essential features of the microscopic model.

The long range correlations (generating fractal behavior) in the dynamical etching process are generated in the regime in which the linear coefficient takes values around its critical value. As a consequence, it is inferred that the fractal properties of the final frozen configuration are related to the standard dynamical percolation renormalization group fixed point in any dimension.

Up to higher order terms, $q(\mathbf{x}, t)$ can be written as $q(\mathbf{x}, t) \propto \int dt' \rho(\mathbf{x}, t')$. This variable, the integral over the past history of the activity field, represents the statistics of immunized sites as described by Janssen [13], and therefore, in our problem the statistics of “surviving” solid clusters in [8,9] is also related to percolation properties. Observe that regions of the cluster of corroded sites far from the final blocking corrosion front have been corroded with a value of p larger than its critical value and therefore are not critical. For the same reason the final corrosion front can be seen as the external perimeter of an invading percolation cluster (the etchant solution) with $p \simeq p_c$. This explains the value of the fractal dimension $D_f \simeq 1.75$ found for this final corrosion front, which is nothing but the hull exponent of percolation in the lattice geometry under consideration [9,22].

Finally, we can perform a finite size scaling analysis of our equation in order to determine how different magnitudes scale as a function of the only free parameter, V ; in particular, we can evaluate the distance from the critical point at which the process will be finally stopped. The linear coefficient in Eq. 14 is

$$\mu(\mathbf{x}, t) = s(\mathbf{x}, 0)p(0) \exp \left[-\frac{1}{V} \int_0^t dt' \int d\mathbf{x}' \rho(\mathbf{x}', t') \right] - c(\mathbf{x}, 0). \quad (15)$$

For the points where the dynamics is arrested, at t_f , it is clear that $s(\mathbf{x}, 0) = 1$ and $c(\mathbf{x}, 0) = 0$; i.e. at $t = 0$ they belong to the solid bulk. Hence, for the bulk we have $\mu(t) = p(0) \exp \left[-\frac{1}{V} \int_0^t dt' \int d\mathbf{x}' \rho(\mathbf{x}', t') \right]$ independent of \mathbf{x} . As usual t_c is the time at which the process is critical $\mu(t_c) = \mu_c$, and t_f the time at which the process is actually arrested. For large values of V the argument of the exponential in Eq. 15 can be expanded in power series, and we have, up to the leading order:

$$\mu(t_c) - \mu(t_f) \propto \frac{1}{V} \int_{t_c}^{t_f} dt' \int d\mathbf{x}' \rho(\mathbf{x}', t'). \quad (16)$$

Now we can use the scaling analysis presented in the first part of the paper. In the time interval between t_c and t_f the solution erodes a region of the solid with, roughly speaking the shape of a circular hole limited by a crown of radius R_c and width σ . As argued before $R_c \propto \sqrt{V}$. Moreover, since the quantity $\int_{t_c}^{t_f} dt' \int d\mathbf{x}' \rho(\mathbf{x}', t')$ gives the amount of material tested by the etching solution between t_c and t_f , we can write $\int_{t_c}^{t_f} dt' \int d\mathbf{x}' \rho(\mathbf{x}', t') \sim R_c \sigma$. Therefore $\mu(t_c) - \mu(t_f) \propto \sigma/\sqrt{V}$. Writing $\sigma \propto (1/\sqrt{V})^{-\alpha_\sigma}$ one obtains

$$\mu(t_c) - \mu(t_f) \propto \left(\sqrt{V} \right)^{\alpha_\sigma - 1}. \quad (17)$$

The fact that V is finite then implies that σ is finite and $\mu(t_c) - \mu(t_f) \neq 0$. It is only in the large V limit that the process is stopped exactly at the dynamical percolation critical point. As discussed in section 3, one has $\alpha_\sigma = 1/D_f$ [9,22], and therefore the distance from the final mass to the critical one scales as Δp , that is as the excursion of the occupancy probabilities along the separation interface of GP. Therefore we have determined not only the universality class, but also established how finite size effect operate in the DEM.

In conclusion, all the critical (fractal) properties of the microscopic model can be shown to be related to (dynamical) percolation in any space dimension, by using the above presented continuous (field theoretical) representation, and finite size corrections can be evaluated.

V. CONCLUSIONS

Summing up, we have found that the dynamical etching model proposed by Sapoval et al., is a self-organized process describable by a the continuous Langevin equation similar to that of dynamical percolation. This Langevin equation includes a linear term coefficient that decreases monotonously as the etching process goes on. In this way as soon as it takes its critical value and enters

the “absorbing” regime the etching process is stopped. Consequently, the fractal (scale invariant) properties of the interface in the etching process are shown to be related to the (dynamical) percolation renormalization group fixed point. This result is valid in any space dimension. In particular, our analysis permits us to conclude that the etching upper critical dimension is $d_c = 6$, as in (dynamical) percolation. On the other hand, we have also evaluated the role of finite size corrections that are essentially different from those of standard dynamical percolation.

An interesting aspect from a theoretical perspective is that the field theory (Langevin equation) describing the process is self-organized, in the sense that, without any parameter fine-tuning, fractal, scale-invariant properties are generated. However, it is only in the limit $V \rightarrow \infty$ ($1/V \rightarrow 0$), that the upper cut-off for scaling diverges. This is in clear analogy with what occurs in other models of self-organization, as sandpiles [27] for which critical behavior is observed in the limit of dissipation and driving going to zero [28].

The mechanism discussed in this paper constitutes a new “path” to self-organized criticality [10], in which the control parameter decreases monotonously until it reaches the neighborhood of the absorbing-state phase transition at which the dynamics is arrested in an exponential way. This same mechanism will be investigated in the context of different types of absorbing-state phase transitions (as directed percolation [15,16]) in a future work. Observe that this scenario has the great advantage of being related in a clear-cut way to real physical systems, making therefore the observation of self-organized criticality much more accessible to experiments.

ACKNOWLEDGMENTS

We acknowledge useful discussion with A. Baldassarri, U. Marini Bettolo Marconi and P. Hurtado. We acknowledge partial support from the European Network contract ERBFMRXCT980183, and DGESIC (Spain) project PB97-0842. We thank It. FFSS for giving us the opportunity to discuss this problem. M.A.M. acknowledges the kind hospitality at the Ecole Polytechnique where this work was started.

-
- [1] U. R. Evans, *The corrosion and Oxidation of Metals: Scientific Principles and Practical Applications*, Arnold, (London), 1960). H. H. Uhlig, *Corrosion and Corrosion Control*, (Wiley, New York), 1963.
 [2] B. Mandelbrot, *The fractal Geometry of Nature*, (Freeman, San Francisco, 1982).
 [3] P. Meakin, *Fractals, scaling and growth far from equilib-*

rium, Cambridge Nonlinear Science Series 5, (Cambridge University Press), 1998.

- [4] A. L. Barabasi and H. E. Stanley, *Fractal Concepts in Surface Growth*, (Cambridge University press, Cambridge, 1995).
 [5] T. Halpin-Healy and Y.-C. Zhang, *Phys. Rep.* **254**, 215 (1995).
 [6] *Percolation Structures and Processes*, edited by G. Deutscher, R. Zallen, and J. Adler, Annals of the Israel Physical Society, Vol. 5 (Adam Hilger, Bristol), 1983.
 [7] L. Balázs, *Phys. Rev. E* **54**, 1183 (1996).
 [8] B. Sapoval, S. B. Santra, and P. Barboux, *Europhys. Lett.*, **41**, 297, (1998). S. B. Santra and B. Sapoval, *Physica A* **266**, 160 (1999).
 [9] A. Gabrielli, A. Baldassarri, and B. Sapoval, *Phys. Rev. E.* **62**, 3103 (2000).
 [10] R. Dickman, M. A. Muñoz, A. Vespignani, and S. Zapperi, *Brazilian J. of Physics* **30**, 27 (2000).
 [11] Observe that at early times $p(t)$ has to be larger than percolation threshold p_c ; otherwise the dynamics comes to its end without reaching a critical regime.
 [12] J.L. Cardy, *J. Phys. A* **16**, L709 (1983); J.L. Cardy and P. Grassberger, *J. Phys. A* **18**, L267 (1985).
 [13] H.K. Janssen, *Z. Phys. B* **58**, 311 (1985).
 [14] In the language of excitable media (autocatalytic chemical reactions, propagation of electrical activity in neurons, spreading of diseases) there are, in general three types of states called: quiescent (healthy), excited (infected), and refractory (immune).
 [15] J. Marro and R. Dickman, *Nonequilibrium Phase Transitions in Lattice Models*, (Cambridge University Press, Cambridge, 1999).
 [16] See, G. Grinstein and M. A. Muñoz, *The Statistical Mechanics of Systems with Absorbing States*, in “Fourth Granada Lectures in Computational Physics”, edited by P. Garrido and J. Marro, Lecture Notes in Physics, Vol. 493 (Springer, Berlin 1997), p. 223, and references therein. See also, H. Hinrichsen, *Adv. Phys.* **49**, 815 (2000).
 [17] R. Bausch, H. K. Janssen, and H. Wagner, *Z. Phys. B* **24**, 113 (1976). C. De Dominicis and L. Peliti, *Phys. Rev. B* **18**, 353 (1978).
 [18] D. J. Amit, *Field Theory, the Renormalization Group and Critical Phenomena*, (World Scientific, Singapore, 1992). J. Zinn-Justin, *Quantum Field Theory and Critical Phenomena*, (Clarendon Press, Oxford, 1990).
 [19] T. C. Lubensky and J. Isaacson, *Phys. Rev. Lett.* **41**, 829 (1978); *Phys. Rev. A* **20**, 2130 (1979).
 [20] B. Sapoval, M. Rosso, and J. F. Gouyet, *J. Phys. Lett. (Paris)*, **46**, L149 (1985); B. Sapoval, M. Rosso, and J. F. Gouyet, in *The Fractal Approach to Heterogeneous Chemistry*, edited by D. Avnir (John Wiley and Sons Ltd., New York, 1989). M. Rosso, J. F. Gouyet, and B. Sapoval, *Phys. Rev. B* **32**, 6053 (1985).
 [21] R. Ziff and B. Sapoval, *J. Phys. A : Math. Gen.* **19**, L1169-1172 (1986). The connectivity criterion is a relevant ingredient to be taken in consideration. For example, in a square lattice, the connection between occupied sites is to first neighbor while the connection between empty (etched) sites is to first and second nearest neighbors. See

- the discussion in [9].
- [22] H. Saleur and B. Duplantier, Phys. Rev. Lett. **58**, 2325 (1986).
 - [23] C. W. Gardiner and S. Chatuverdi, J. Stat. Phys. **17**, 429 (1977); *ibid* **18**, 501 (1978). See also C. W. Gardiner, *Handbook of Stochastic Methods*, Springer-Verlag, Berlin and Heidelberg, 1985.
 - [24] M. A. Muñoz, Phys. Rev. E. **57**, 1377 (1998).
 - [25] L. Peliti, J. Physique **46**, 1469 (1985). See also, B. P. Lee and J. Cardy, J. Stat. Phys. **80**, 971 (1995).
 - [26] Observe that the critical value of the linear term coefficient is equal to zero only at mean field (tree) level. As soon as fluctuations, i.e. diagrammatic corrections, are taken into account the critical mass is shifted to a non-vanishing value [12,13].
 - [27] P. Bak, C. Tang and K. Wiesenfeld, Phys. Rev. Lett. **59**, 381 (1987); Phys. Rev. A **38**, 364 (1988).
 - [28] A. Vespignani, R. Dickman, M. A. Muñoz, and S. Zapperi, Phys. Rev. E **62**, 4564 (2000).